

Xylem- and Phloem-Based Transport of CuO Nanoparticles in Maize (*Zea mays* L.)

Zhenyu Wang,[†] Xiaoyan Xie,[†] Jian Zhao,[‡] Xiaoyun Liu,[§] Wenqiang Feng,[†] Jason C. White,^{||} and Baoshan Xing^{*,‡}

[†]College of Environmental Science and Engineering, Ocean University of China, Qingdao 266100, People's Republic of China

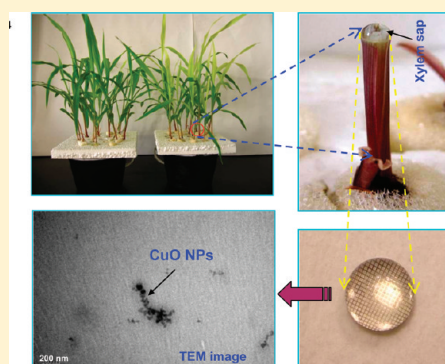
[‡]Department of Plant, Soil and Insect Sciences, University of Massachusetts, Amherst, Massachusetts 01003, United States

[§]Institute of Materials Science and Engineering, Ocean University of China, Qingdao 266100, People's Republic of China

^{||}Department of Analytical Chemistry, Connecticut Agricultural Experiment Station, New Haven, Connecticut 06511, United States

S Supporting Information

ABSTRACT: This work reports on the toxicity of CuO nanoparticles (NPs) to maize (*Zea mays* L.) and their transport and redistribution in the plant. CuO NPs (100 mg L⁻¹) had no effect on germination, but inhibited the growth of maize seedlings; in comparison the dissolved Cu²⁺ ions and CuO bulk particles had no obvious effect on maize growth. CuO NPs were present in xylem sap as examined by transmission electron microscopy (TEM) and energy dispersive spectroscopy (EDS), showing that CuO NPs were transported from roots to shoots via xylem. Split-root experiments and high-resolution TEM observation further showed that CuO NPs could translocate from shoots back to roots via phloem. During this translocation, CuO NPs could be reduced from Cu (II) to Cu (I). To our knowledge, this is the first report of root–shoot–root redistribution of CuO NPs within maize. The current study provides direct evidence for the bioaccumulation and biotransformation of CuO NPs (20–40 nm) in maize, which has significant implications on the potential risk of NPs and food safety.



INTRODUCTION

Engineered nanoparticles (NPs) are widely used in industrial and commercial products and have likely entered the environment, causing potentially adverse effects on ecosystem structure and function.^{1,2} As novel and emerging toxicants, NP ecotoxicity is a topic receiving increased scrutiny from both the scientific and regulatory communities.

Plants are a critical component of ecosystems, serving both as important ecological receptors and as a potential pathway for NP transport and bioaccumulation into food chains.³ Currently, a number of studies have demonstrated NP toxicity to plant species. NPs have been shown to reduce ryegrass (*Lolium perenne*) and *Arabidopsis* (*Arabidopsis thaliana*) seedling growth and alter root morphology under hydroponic conditions.^{4–6} ZnO NPs were shown to enter ryegrass (*Lolium perenne*) cells and were able to pass through the epidermis and cortex via apoplastic pathway.⁴ Magnetization was detected in the roots and leaves of the pumpkin plants exposed to Fe₃O₄ NPs in the growth media.³ Similarly, Lin et al.⁷ reported C₇₀ uptake and accumulation in rice plants, as well as in the seedlings of the next generation. Whereas multiwalled carbon nanotubes directly penetrated periwinkle (*Catharanthus roseus*) protoplasts,⁸ single-walled carbon nanotubes labeled with fluorescein isothiocyanate entered Bright Yellow (BY-2) cells through endocytosis.⁹ Carbon-coated magnetic NPs could be taken up by the roots of crops (pea, sunflower, tomato, and wheat) and

distributed in the whole plant.¹⁰ Although these studies have advanced our understanding of plant-nanoparticle interactions, the mechanisms of NPs transport between root and shoot, and the definitive evidence of the transformation of NPs in the plant tissues are still lacking.

CuO NPs are used extensively in commercial applications, including gas sensors, photovoltaic cells, heat transfer nanofluids, magnetic phase transitions, catalysts, and semiconductors.^{11,12} Toxicity of CuO NPs to aquatic organisms (e.g., fish, alga) has been observed.^{13–15} For the terrestrial plants, although CuO NPs uptake by wheat¹⁶ and toxicity to ryegrass and radish¹⁷ have been reported, knowledge on the transport and fate of CuO NPs in the plant remains limited, and there is no research focusing on maize, a major agricultural crop. Therefore, the objectives of the present work were to (1) investigate the toxicity of CuO NPs to maize during germination and seedling growth; (2) examine the uptake of CuO NPs in maize seedlings, including the localization and distribution of the NPs in seedling tissues and cells, and (3) obtain mechanistic information on CuO NP translocation and

Received: November 23, 2011

Revised: March 16, 2012

Accepted: March 21, 2012

Published: March 21, 2012

accumulation in maize seedlings through xylem sap extraction and split-root experiments.

MATERIALS AND METHODS

Nanoparticle Suspension Preparation and Characterization. CuO NPs and bulk particles (BPs) were purchased from Beijing Nachen Sci & Tech Co., P. R. China. The morphology of the CuO NPs and BPs was examined using transmission electron microscopy (TEM, JEM-2100, Japan) operated at 200 kV. The characteristics of CuO NPs (20–40 nm) and BPs (1500 nm) are shown in Table S1 and Figure S1 of the Supporting Information, SI.

The dissolution kinetics of CuO NPs was determined in 25% strength of the nutrient solution (see below). One hundred mg L⁻¹ CuO NPs were added to this diluted nutrient solution and agitated by ultrasonic vibration (100 W, 40 kHz) for 30 min to increase dispersion. At 1 h, 3 h, 9 h, 24 h, and 72 h, suspensions were centrifuged (10 000 rpm for 30 min) and filtered (0.22 μ m glass filter). Cu²⁺ ion concentration in the supernatant was determined by flame atomic absorption spectrophotometry (AAS) (Solaar M 6, Thermo Electron).

Seed Germination and Root Elongation. Maize seeds (*Zea mays* L. cv. Yudan No. 8) were purchased from Qingdao seed station. Seeds were immersed in a 10% H₂O₂ solution for 10 min and then rinsed three times with deionized water to ensure surface sterility. In a preliminary study, the average germination rate of maize seeds was greater than 85%. The seeds were then immersed in deionized water, Cu²⁺ solution (0.15 mg L⁻¹), CuO BPs (100 mg L⁻¹), or NP suspension (2, 5, 10, 20, 30, 40, 50, 100 mg L⁻¹) for approximately 2 h.¹⁸ The seeds were subsequently placed in Petri dishes (100 mm \times 15 mm); there were 10 seeds per dish spaced at approximately 1 cm intervals. Every dish was then amended with 5 mL test medium containing CuO NPs, Cu²⁺ ions and CuO BPs, as mentioned above, and covered in the dark at 25 °C. Germination was quantified when the bud length surpassed half of the seed length. In addition, root length was measured over the course of 8 days.

Hydroponic Culture. Maize seedlings were germinated after surface sterilization and were immersed in deionized water. Uniform seedlings were selected and transferred into plastic containers amended with 25% strength of the following nutrient solution (mmol L⁻¹): K₂SO₄, 0.75; Ca(NO₃)₂, 2.0; KCl, 0.1; KH₂PO₄, 0.25; MgSO₄·7H₂O, 0.65; H₃BO₃, 1.0 \times 10⁻³; MnSO₄·H₂O, 1.0 \times 10⁻³; ZnSO₄·7H₂O, 1.0 \times 10⁻³; CuSO₄·5H₂O, 1 \times 10⁻⁴; (NH₄)₆Mo₇O₂₄, 5 \times 10⁻⁶; Fe-EDTA, 0.1. The pH of the nutrient solution was adjusted to 6.8. The seedlings were grown for 15 days at 20–25/15–20 °C (day/night) with relative humidity 60%–70%, and a light intensity of 16 500 lx. After appearance of the third leaf, five treatment groups were initiated: 10 mg L⁻¹ and 100 mg L⁻¹ CuO NPs, 100 mg L⁻¹ CuO BPs, Cu²⁺ ions and control. The particles and ions were suspended and dissolved in 25% strength nutrient solution. The phytotoxicity experiment lasted for 15 days and the suspensions and dissolved solutions were renewed every 3 days. After exposure for 15 days, the seedlings were washed with tap water followed by three rinses with deionized water. Shoot and root tissues were separated and the fresh weight was measured. The roots were scanned and morphological parameters were analyzed with the WinRHIZO Pro 2005 b (Regent Instruments Inc., Canada). Dry biomass was the determined after drying at 70 °C for 24 h. The Cu contents in

the shoots and roots of tissues from all treatments were measured by flame AAS after HNO₃ digestion.¹⁹

TEM Observation. Fresh maize roots were thoroughly washed with deionized water. Maize root samples were prefixed in 5% glutaraldehyde, washed in 0.1 mol L⁻¹ pH 7.2 phosphate buffer, postfixed in 1% osmium tetroxide for 2 h, dehydrated in a graded series of ethanol, and embedded in epoxy resin (ETON 812). Samples were sectioned to 60–80 nm thick using an Ultracut E Microtome (LKB Novoa) and stained with uranyl acetate. The root tissues were then placed on Ni-based grids instead of Cu so as to avoid elemental interference during TEM with energy dispersive spectroscopy (EDS, INCA100, Oxfordshire, U.K.).

K⁺ Leakage Rate. The measurement of potassium leakage was determined using the procedure of Navari-Izzo et al.²⁰ The shoot and root systems of seedlings from each treatment were separated and washed with deionized water three times to remove cellular debris. Roots and shoots were incubated in 50 mL of deionized water and shaken at 21 °C for 4 h. Aliquots of each sample were then taken for K determination by flame AAS.

Xylem Sap Extraction In Situ. Xylem sap was collected by the procedure Buhtz et al.²¹ After 15-day-long exposure to 0.15 mg L⁻¹ Cu²⁺ ions or 100 mg L⁻¹ CuO NPs as described above, xylem samples were obtained by severing the stems of maize seedlings about 5 cm above the surface of the nutrient solution. After thorough washing of the stem surface on the root side with deionized water, the tissues were blotted dry and the exuding fluid was collected and deposited on a Ni grid and then was analyzed by TEM to determine the CuO NPs presence.

Split-Root Techniques. The split-root container system was used as shown in Figure S2 of the SI. One side container was amended with deionized water, and the other side container was amended with 100 mg L⁻¹ CuO NPs or 0.15 mg L⁻¹ Cu²⁺ in deionized water.²² The roots of one seedling were manually separated into two parts and carefully placed in the two separate containers. The seedlings were harvested after two days exposure and the Cu contents in the roots and shoots were measured as described.¹⁹ TEM samples of the leaves and the roots in the container filled with deionized water were prepared as above.

Statistical Analysis. All treatments had a minimum of three replicates, with results presented as mean \pm SD (standard deviation). Statistical analysis was performed using one-way analysis of variance (ANOVA) with the Fisher LSD post hoc test. Differences were considered statistically significant when p < 0.05.

RESULTS AND DISCUSSION

Effects of CuO NPs on Germination and Root Elongation. Cu²⁺ ions were released in the CuO NPs suspension and the equilibrium concentration was 0.11 mg L⁻¹ (Figure S3 of the SI). In order to investigate the contribution of ions released from CuO NPs to the observed phytotoxicity, 0.15 mg L⁻¹ Cu²⁺ ions were included as a treatment in the experimental design.

At day 6 of the germination experiment, germination rates were not significantly different among all the treatments (p < 0.05) (Figure S4 of the SI). These findings are in agreement with Lin and Xing and Stampoulis et al.,^{18,23} both of whom observed that seed germination is generally an insensitive measure of phytotoxicity from NPs. This observation may be due to seed coat selective permeability, relatively short exposure

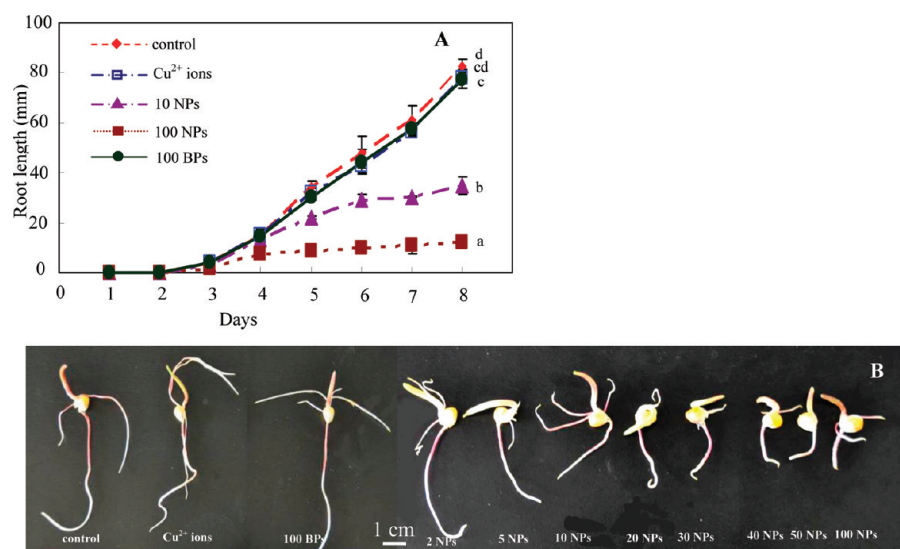


Figure 1. Root length of maize during 8-day CuO NPs exposure. (A) Root length in the presence of 10 mg L⁻¹ CuO NPs (10 NPs), 100 mg L⁻¹ CuO NPs (100 NPs), 0.15 mg L⁻¹ Cu²⁺ ions and 100 mg L⁻¹ CuO BPs (100 BPs) during 8 days. The values were given as mean \pm SD of triplicate samples with 10 seedlings each. Different letters represent significant differences between the treatment means ($p < 0.05$, LSD); (B) Photos of maize seedlings incubated in 0.15 mg L⁻¹ Cu²⁺ ions, 100 mg L⁻¹ CuO BPs and 0–100 mg L⁻¹ CuO NPs after 8 days germination.

times, or other uncharacterized biological processes. Conversely, the root elongation of maize was significantly inhibited by 10 and 100 mg L⁻¹ CuO NPs (Figure 1) relative to BP, ion, and unexposed controls. By the second day of the root elongation assay (8 days after the initial germination assay), values for the control, 10 mg L⁻¹ CuO NPs and 100 mg L⁻¹ CuO NPs were significantly different ($p < 0.01$). Exposure to 10 and 100 mg L⁻¹ CuO NPs reduced root elongation by 55% and 84% respectively, relative to unexposed, Cu²⁺ ions, and bulk controls ($p < 0.01$). Notably, the inhibition of root length is CuO NP concentration-dependent (Figure 1B). Exposure to Cu²⁺ ions and 100 mg L⁻¹ CuO BPs treatment had no impact on root elongation as compared to unexposed control plants ($p < 0.05$). The reason for a significant phytotoxic effect on root elongation relative to seed germination likely relates to the fact that after penetration of the seed coats, the emerging radicles rapidly absorb nutrients and water, therefore maximizing particle exposure.

Phytotoxicity of CuO NPs to the Seedlings of Maize. By the emergence of the third leaf, plants exposed to CuO NPs had developed chlorotic symptoms (Figures 2A and S5 of the SI). Root and shoot biomass was impacted significantly in all CuO NPs treatments as compared to bulk, ion and unexposed control plants (Figures 2 and S6 of the SI). The observed toxicity was dependent on CuO NP concentration and exposure time. By day 14, 10 mg L⁻¹ CuO NPs reduced the fresh weight of root and shoot tissues by 60% and 34% respectively, compared to the unexposed control plants. Similarly, 100 mg L⁻¹ CuO NP treatment significantly reduced maize biomass (root/shoot fresh and dry weight) as compared to controls ($p < 0.05$); there were no differences between the unexposed, Cu²⁺ ions and BPs controls. The results demonstrated that root tissues were more sensitive to CuO NPs than were the shoots; this is not surprising given that roots interact with NPs directly. Root morphology was further examined. Root length and root surface area were reduced significantly by CuO NP exposure as compared to the bulk, ion and unexposed treatments, whereas the average diameter of root was increased (Table S2 of the SI). The similar changes of

root length and diameter were observed on *Arabidopsis thaliana* when exposed to TiO₂ NPs²⁴ and fullerene.²⁵ This aberrant root morphology is a stress resistance of plants, and hormones may act as an intermediate factor,^{25–27} as a result, cellulose microfibrils in the parenchyma cell walls were axially deposited. The disruption of microtubule networks may be another reason for the aberrant root morphology by NPs, which could lead to the isotropic growth of cells and the swelling of roots.^{24,25} The moisture content of maize roots and shoots decreased significantly upon 100 mg L⁻¹ CuO NP exposure after 8 days (Figure S7 of the SI). Asli and Neumann²⁸ reported that TiO₂ NPs could reduce the hydraulic conductivity of maize roots, and induce symptoms of water stress in shoots. This may be also the reason of the moisture content decrease after CuO NP exposure. As such, the decreased root and shoot biomass of maize seedlings was in part due to the resulting decrease in water uptake. CuO BP and Cu²⁺ ion treatments showed no significant impact on maize seedling growth ($p < 0.05$). Importantly, it can be concluded that the concentration of solubilized Cu²⁺ ions released from CuO NPs was not sufficient to cause toxicity and that the observed negative physiological effects are in fact due to the elemental CuO NPs themselves.

Uptake of CuO NPs in Plant. Plants are a potential pathway for the bioaccumulation of NPs into the food chain and through ecosystems.²⁹ Figure 3A shows the Cu content of maize roots and shoots after 14 days exposure to Cu²⁺, CuO NP and corresponding BPs. The contents in plant tissues increased with increasing NP concentrations. With the exception of 100 mg L⁻¹ CuO NPs ($p < 0.05$) there were no significant differences in root Cu content across all treatments. The Cu content in the roots of plants exposed to 100 mg L⁻¹ CuO NPs was 3.6 times higher than that of control, 2 times higher than Cu²⁺, and 1.8 times higher than CuO BPs. Similarly, Cu content in the shoots at 100 mg L⁻¹ CuO NPs was 7 times higher than the control, 1.2 times more than Cu²⁺ treatment, and 1.8 times more than BPs. These results indicated that CuO NPs were probably transported to the shoot system from the roots.

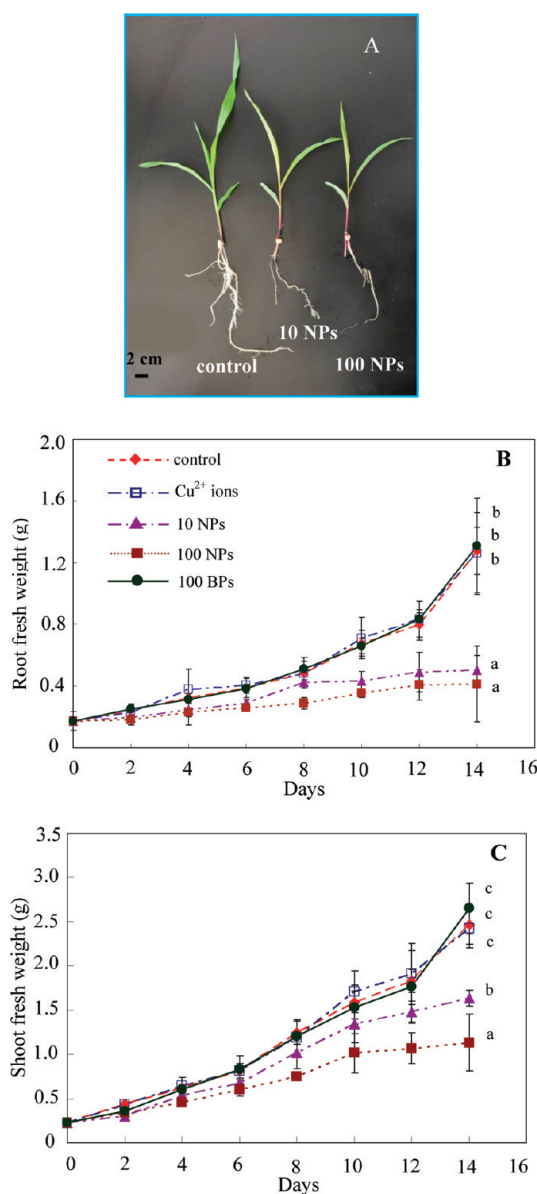


Figure 2. Effects of CuO NPs on maize growth. (A) The growth inhibition of CuO NPs on maize seedlings after cultured for 15 days in the nutrient solutions with CuO NPs. Effect of 10 mg L⁻¹ CuO NPs (10 NPs), 100 mg L⁻¹ CuO NPs (100 NPs), 0.15 mg L⁻¹ Cu²⁺ ions and 100 mg L⁻¹ CuO BPs (100 BPs) on (B) root fresh weight and (C) shoot fresh weight.

Further analysis was performed to confirm the presence of CuO NPs in the root of the maize seedlings. The root tip of 15-day-old maize seedlings exposed to 100 mg L⁻¹ CuO NPs were analyzed by TEM (Figure 4). CuO NPs not only existed inside the cell wall of epidermal cell (Figure 4A,B,F), but also in the intercellular space and cytoplasm of cortical cells (Figure 4C), as well as in the nuclei (Figure 4D,E). Concurrently, the elemental composition of the dark regions in the cells was analyzed by EDS (Figure S8), and the spectra confirmed the presence of Cu. The dark Cu-containing regions were not observed under the unexposed control. The existence of CuO NPs in the intercellular space demonstrates that NPs may pass through the epidermis and cortex via apoplastic pathways. As a confirmation that CuO NPs could enter the cells, it is important to understand the primary transmembrane pathway

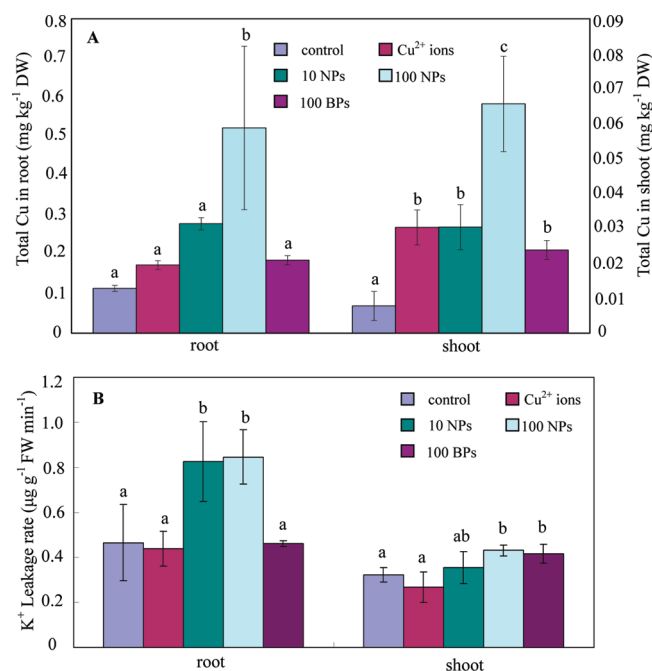


Figure 3. Root/shoot Cu contents in the presence of 0.15 mg L⁻¹ Cu²⁺ ions, 10 mg L⁻¹ CuO NPs (10 NPs), 100 mg L⁻¹ CuO NPs (100 NPs), and 100 mg L⁻¹ CuO BPs (100 BPs) (A). Effects of 0.15 mg L⁻¹ Cu²⁺ ions, 10 mg L⁻¹ CuO NPs (10 NPs), 100 mg L⁻¹ CuO NPs (100 NPs), and 100 mg L⁻¹ CuO BPs (100 BPs) on K⁺ leakage of 15-day-old maize seedlings (B). The values were given as mean ± SD of triplicate samples. Different letters represent significant differences between the treatment means ($p < 0.05$, LSD).

for CuO NPs uptake. In Figure 4G and H, an endosome (~500 nm) was observed. Early endosome has a morphological appearance of tubular-vesicular structure³⁰ rather than the spheroidal structure observed in our study. The size of endosome in Figure 4G and H was similar to the late endosome observed in tobacco BY-2 cells.³⁰ Therefore, the observed endosome was likely a late endosome. The presence of endosome suggests that endocytosis may be one mode of NP entry into plant cells and agrees with our previous study demonstrating that endocytosis permitted uptake of CuO NPs into the alga *Microcystis aeruginosa*.¹⁵

After entering the cells, the NPs may induce the formation of reactive oxygen species (ROS)² and lipid peroxidation, subsequently compromising membrane integrity. To ascertain the effect of CuO NPs on plasma membrane integrity, K⁺ leakage rates from maize roots and shoots were determined (Figure 3B). The loss of root plasma membrane integrity was significantly greater than that in shoot tissues. In the roots, K⁺ leakage rates under CuO NP treatment were significantly higher than that of unexposed controls, ions, or equivalent BP treated plants ($p < 0.05$). Although the membrane was damaged, CuO NPs had already entered the cells without membrane disruption (Figure 4C), confirming particle uptake into the cell by endocytosis.

Xylem-Based Transport of CuO NPs. Higher Cu²⁺ concentration in shoot than unexposed controls, as well as equivalent BP and ion treated plants, indicates CuO NP transport from roots to shoots. Zhang et al.³¹ revealed that ceria NPs could be transferred from the roots to shoots in cucumber plants using a radiotracer method. C₇₀ NPs were hypothesized to enter the roots and to then be transported to the stems and

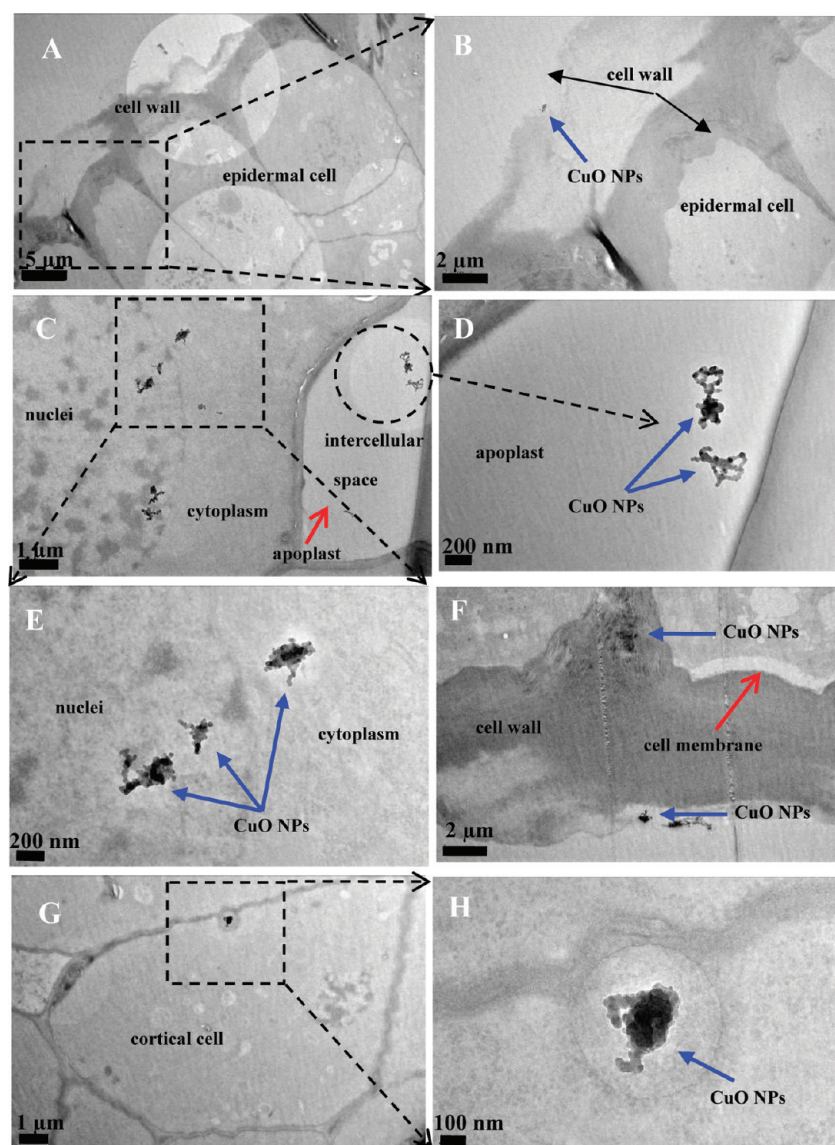


Figure 4. Root uptake of CuO NPs in 15-day-old maize seedlings. Epidermal cell walls entrapped CuO NPs (A, B) and translocation of CuO NPs across epidermal cell walls (F). Magnified view (B) of the region squared in (A). CuO NPs can be seen near the interface between the plant cell wall and the plasma membrane (F). CuO NPs in cell and intercellular space of cortical cells (C–E). Magnified views (D,E) of the circled region and squared region in (C). The corresponding EDS spectra of dark dots for each image are presented in Figure S8. In addition, endocytosis-like structure was observed in the cells (G, H).

leaves of rice plants.⁷ To verify if CuO NPs can move from root to shoot, the xylem sap of maize seedlings (Figure S9 of the SI) exposed to 100 mg L⁻¹ CuO NPs was analyzed by TEM (Figure 5). Several dark regions were present in the nickel grid, and the EDS spectra confirm Cu presence. For the Cu²⁺ treatment, however, no dark Cu-containing regions were observed. To further exclude the possibility of Cu²⁺ ions, the CuSO₄ solution and CuSO₄ solution with xylem sap treatments were set in contrast to the CuO NP treatment (Figure 5A–C). The patterns of the two images were different from the CuO NP treatment, which possessed the dark Cu-containing regions. In addition, the diffraction pattern of the dark regions corresponded to the (110), (002), (−112), and (020) planes of the face-centered cubic structure of CuO, demonstrating that these features consisted of CuO NPs. The presence of CuO NPs in xylem sap provides direct and definitive evidence for the root to shoot transport of CuO NPs. Prior to entry into the vascular cylinder, the CuO NPs in the roots must cross the

endodermis. It is worth noting that the casparian strip, a deposition of suberin between radial cell walls, is specific to the endodermal cells, and is important to the protection of the plant.³² However, at the root apex the casparian strip is not yet fully developed.^{33,34} Therefore, CuO NPs may pass through the root apex and move to the stele, with subsequent transport to the shoots via xylem. The transported NPs may then be unloaded to leaves from the xylem. The Cu²⁺ concentrations were elevated in the shoots/leaves exposed to CuO NPs. More importantly, the presence of CuO NPs was observed in the leaves by TEM (see below in the split-root experiment).

Phloem-Based Transport of CuO NPs. CuO NPs in the leaves may be translocated to other tissues through phloem transport. For example, some metals³⁵ are transferred from the shoots/leaves to roots, but the likelihood of this transport process for NPs is not known. Lin et al.⁷ did show that C₇₀ was transmitted to the progeny of exposed rice plants. As such, a split-root experiment was therefore designed and conducted. A

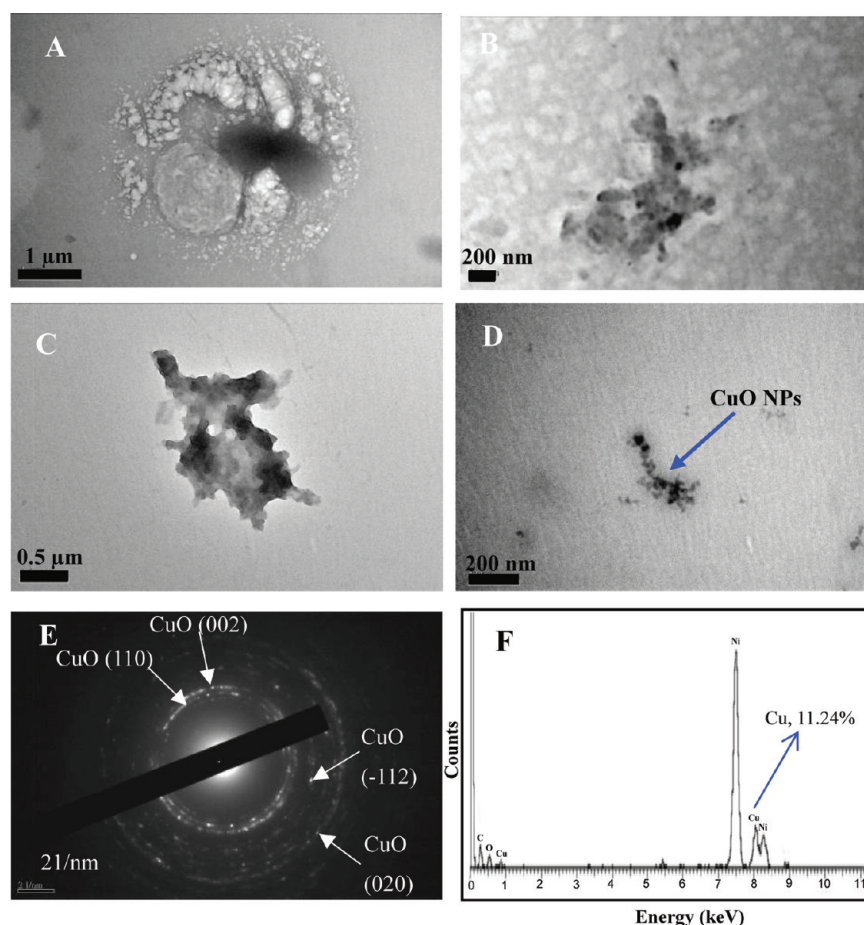


Figure 5. TEM images and crystal structure analysis of CuO NPs in the xylem sap; CuSO₄ solution only (A); xylem sap of Cu²⁺ ions treatment (B); CuSO₄ solution + xylem sap (C); xylem sap of CuO NPs treated seedlings (D); electron diffraction pattern of the dark particles from image D (E); the diffraction pattern showed the diffraction spots corresponding to the (110), (002), (−112), and (020) planes of the face-centered cubic structure of CuO; and EDS spectra (F) of the dark particles from image D. The Ni signal in the spectrum is a result of the TEM Ni grids used for sample examination.

portion of the root system of a single plant was exposed to deionized water, and the other portion was immersed in 100 mg L^{−1} CuO NPs suspension or 0.15 mg L^{−1} Cu²⁺ ions (Figure S2 of the SI). The Cu contents of the roots immersed in deionized water and the shoots were analyzed, respectively. For CuO NPs treatment of the split-root experiment, Cu was detected in both shoots and the roots immersed in the deionized water, and this Cu content was significantly higher than those of shoots and roots in immersed in the deionized water of the control and the Cu²⁺ ions treatments of the split-root experiment ($p < 0.05$) (Figure 6A), indicating that CuO NPs may be present in the shoots and the roots immersed in the deionized water. Importantly, CuO NPs were observed in the leaf cells after treated by CuO NPs in the split-root system (Figure S10 of the SI). Moreover, TEM analysis revealed the presence of familiar dark aggregates in the roots indirectly exposed to CuO NPs (Figures 6B and S11 of the SI), showing that CuO NPs could be transported from shoots to roots through phloem. The mechanism for this phloem transport system remains unknown but NPs may be associated with carbohydrates³⁶ during normal photosynthate storage activities.

Upon further analysis of dark aggregates in the roots (i.e., water side) indirectly exposed to CuO NPs by high resolution TEM (HRTEM), there was visible lattice fringe in the root tissues. Interplanar crystal spacing was calculated by fast Fourier

transformation (FFT); the image in Figure 6D represents the FFT patterns of the regions shown in Figure 6C. Interplanar crystal spacing was determined to be 0.3057, 0.2376, and 0.3228 nm, which corresponds to Cu₂O, CuO and Cu₂S, respectively. This demonstrates that some of the CuO NPs were reduced to Cu₂O and Cu₂S in the plant. Enzymes such as the reductases and ferredoxins of the photosynthetic system of the plant³⁷ could reduce Cu (II) to Cu (I). We reported similar CuO NP reduction to Cu₂O in the alga *Microcystis aeruginosa*.¹⁵ Another explanation for the reduction of Cu (II) to Cu (I) may be related to the presence of reducing sugars. Carbohydrates in the plant are transported from photosynthetic cells to root tissues.³⁸ These carbohydrates include sugars such as glucose and fructose that can serve as reducing agents. This is supported by Beattie and Haverkamp,³⁶ who described Ag⁺ and Au³⁺ reduction to Ag⁰ and Au⁰ by sugars in *Brassica juncea*. The potential mechanism of Cu₂S is a topic of ongoing study.

In summary, CuO NPs had no obvious inhibition on the germination of maize seeds. However, the NPs at 100 mg L^{−1} induced visible chlorosis and had significant inhibition on seedling growth. No equivalent phytotoxicity of the dissolved Cu²⁺ or corresponding BPs was evident. The CuO NPs in roots could pass through the epidermis and cortex, reaching the stele. Endocytosis is likely one transmembrane pathway for CuO NP uptake. Upon entering the stele, the CuO NPs were

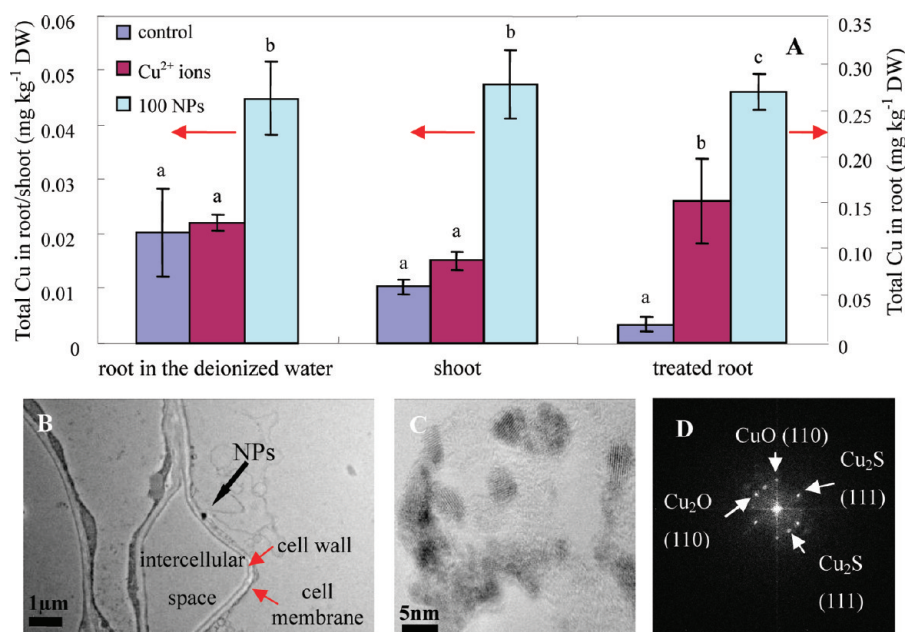


Figure 6. The Cu contents of roots and shoot in the split-root experiment and the TEM observation of CuO NPs in the root. (A) The Cu contents of roots in the deionized water (left Y axis), shoots (left axis) and treated roots (right axis) in the split-root system under 100 mg L⁻¹ CuO NPs (100 NPs) or 0.15 mg L⁻¹ Cu²⁺ ions treatment for 2 days. The values were given as mean \pm SD of triplicate samples. Different letters represent significant differences between the treatment means ($p < 0.05$, LSD). (B) TEM observations of ultrathin slices of *Zea mays* L. root on the side without CuO NPs treatment in the split-root system. HRTEM image (C) was selected from the point with arrows in (B). Representative FFT power spectra (D) were further determined from image (C), CuO, Cu₂O, and Cu₂S interplanar crystal spacing signals were detected from image (D).

transported to shoots via xylem but more importantly, they could be translocated from shoots back to roots via phloem. During this translocation, some of the CuO NPs were reduced from Cu (II) to Cu (I) (Figure S12 of the SI). The molecular mechanisms of CuO NP uptake and transport in the higher plants are, as yet, largely unexplored. To our knowledge, this is the first report of root-shoot-root redistribution of CuO NPs within maize. If accumulated NPs are subsequently released by crop species via root exudation to the rhizosphere, then the resulting implications on plant–microbe process such as nitrogen cycling and nutrient turnover could be significant. The current study provides direct evidence for the biotransformation and bioaccumulation of CuO NPs in maize, which shows the potential risk of NPs in food crops and to human health.

■ ASSOCIATED CONTENT

● Supporting Information

Characteristics and TEM micrographs of particles (Table S1 and Figure S1); schematic display of the split-root system (Figure S2); root morphology (Table S2); time-dependent dissolution of CuO NPs (Figure S3); effect of CuO NPs on germination rates (Figure S4); photos of maize seeding (Figure S5); shoot and root biomass (Figure S6); water content in root/shoot (Figure S7); energy-dispersive spectroscopy analysis (Figure S8); photos of the extract from xylem sap (Figure S9); TEM observation of leaf (Figure S10) and root (Figure S11) in the split-root system; schematic diagram of CuO NPs uptake and translocation (Figure S12). This material is available free of charge via the Internet at <http://pubs.acs.org>.

■ AUTHOR INFORMATION

Corresponding Author

*Tel.: +1 (413) 545-5212; fax: +1 (413) 545-3958; e-mail: bx@pssci.umass.edu.

Notes

The authors declare no competing financial interest.

■ ACKNOWLEDGMENTS

This research was supported by National Natural Science Foundation of China (41073067, 41120134004), Shandong Excellent Young Scientist Program (BS2010HZ023), USDA-AFRI (2011-67006-30181), and USDA-AFRI Hatch program (MAS 00978).

■ REFERENCES

- (1) Moore, M. N. Do nanoparticles present ecotoxicological risks for the health of the aquatic environment? *Environ. Int.* **2006**, *32*, 967–976.
- (2) Nel, A.; Xia, T.; Madler, L.; Li, N. Toxic potential of materials at the nanolevel. *Science* **2006**, *311*, 622–627.
- (3) Zhu, H.; Han, J.; Xiao, J. Q.; Jin, Y. Uptake, translocation, and accumulation of manufactured iron oxide nanoparticles by pumpkin plants. *J. Environ. Monitor.* **2008**, *10*, 713–717.
- (4) Lin, D.; Xing, B. Root uptake and phytotoxicity of ZnO nanoparticles. *Environ. Sci. Technol.* **2008**, *42*, 5580–5585.
- (5) Liu, Q.; Zhao, Y.; Wan, Y.; Zheng, J.; Zhang, X.; Wang, C.; Fang, X.; Lin, J. Study of the inhibitory effect of water-soluble fullerenes on plant growth at the cellular level. *ACS Nano* **2010**, *4*, 5743–5748.
- (6) Kurepa, J.; Paunesku, T.; Vogt, S.; Arora, H.; Rabatic, B. M.; Lu, J.; Wanzer, M. B.; Woloschak, G. E.; Smalle, J. A. Uptake and distribution of ultrasmall anatase TiO₂ alizarin red S nanoconjugates in *Arabidopsis thaliana*. *Nano Lett.* **2010**, *10*, 2296–2302.
- (7) Lin, S.; Reppert, J.; Hu, Q.; Hudson, J.; Reid, M.; Ratnikova, T.; Rao, A.; Luo, H.; Ke, P. Uptake, translocation, and transmission of carbon nanomaterials in rice plants. *Small* **2009**, *5*, 1128–1132.

- (8) Serag, M. F.; Kaji, N. Trafficking and subcellular localization of multiwalled carbon nanotubes in plant cells. *ACS Nano* **2011**, *5*, 493–499.
- (9) Liu, Q. L.; Chen, B.; Wang, Q. L.; Shi, X. L.; Xiao, Z. Y.; Lin, J. X.; Fang, X. H. Carbon nanotubes as molecular transporters for walled plant cells. *Nano Lett.* **2009**, *9*, 1007–1010.
- (10) Cifuentes, Z.; Custardoy, L.; de la Fuente, J.; Marquina, C.; Ibarra, M. R.; Rubiales, D.; Perez-de-Luque, A. Absorption and translocation to the aerial part of magnetic carbon-coated nanoparticles through the root of different crop plants. *J. Nanobiotechnology* **2010**, *8*, 26.
- (11) Zhu, J.; Li, D.; Chen, H.; Yang, X.; Lu, L.; Wang, X. Highly dispersed CuO nanoparticles prepared by a novel quick-precipitation method. *Mater. Lett.* **2004**, *58*, 3324–3327.
- (12) Blinova, I.; Ivask, A.; Heinlaan, M.; Mortimer, M.; Kahru, A. Ecotoxicity of nanoparticles of CuO and ZnO in natural water. *Environ. Pollut.* **2010**, *158*, 41–47.
- (13) Zhao, J.; Wang, Z.; Liu, X.; Xie, X.; Zhang, K.; Xing, B. Distribution of CuO nanoparticles in juvenile carp (*Cyprinus carpio*) and their potential toxicity. *J. Hazard. Mater.* **2011**, *197*, 304–310.
- (14) Ivask, A.; Bondarenko, O.; Jephthina, N.; Kahru, A. Profiling of the reactive oxygen species-related ecotoxicity of CuO, ZnO, TiO₂, silver and fullerene nanoparticles using a set of recombinant luminescent *Escherichia coli* strains: Differentiating the impact of particles and solubilised metals. *Anal. Bioanal. Chem.* **2010**, *398*, 701–716.
- (15) Wang, Z.; Li, J.; Zhao, J.; Xing, B. Toxicity and internalization of CuO nanoparticles to prokaryotic alga *Microcystis aeruginosa* as affected by dissolved organic matter. *Environ. Sci. Technol.* **2011**, *45*, 6032–6040.
- (16) Zhou, D.; Jin, S.; Li, L.; Wang, Y.; Weng, N. Quantifying the adsorption and uptake of CuO nanoparticles by wheat root based on chemical extractions. *J. Environ. Sci.* **2011**, *23*, 1852–1857.
- (17) Atha, D. H.; Wang, H.; Petersen, E. J.; Cleveland, D.; Holbrook, R. D.; Jaruga, P.; Dizdaroglu, M.; Xing, B.; Nelson, B. C. Copper oxide nanoparticle mediated DNA damage in terrestrial plant models. *Environ. Sci. Technol.* **2012**, *46*, 1819–1827.
- (18) Lin, D.; Xing, B. Phytotoxicity of nanoparticles: Inhibition of seed germination and root growth. *Environ. Pollut.* **2007**, *150*, 243–250.
- (19) Sawhney, B. L.; Frink, C. R. Heavy metals and their leachability in incinerator ash. *Water Air Soil Poll.* **1991**, *57–58*, 289–296.
- (20) Navari-Izzo, F.; Izzo, R.; Quartacci, M. F.; Lorenzini, G. Growth and solute leakage in *Hordeum vulgare* exposed to long-term fumigation with low concentrations of SO₂. *Physiol. Plant.* **1989**, *76*, 445–450.
- (21) Buhtz, A.; Kolasa, A.; Arlt, K.; Walz, C.; Kehr, J. Xylem sap protein composition is conserved among different plant species. *Planta* **2004**, *219*, 610–618.
- (22) Schortemeyer, M.; Feil, B.; Stamp, P. Root morphology and nitrogen uptake of maize simultaneously supplied with ammonium and nitrate in a split-root system. *Ann. Bot.* **1993**, *72*, 107–115.
- (23) Stampoulis, D.; Sinha, S. K.; White, J. C. Assay-dependent phytotoxicity of nanoparticles to plants. *Environ. Sci. Technol.* **2009**, *43*, 9473–9479.
- (24) Wang, S.; Kurepa, J.; Smalle, J. A. Ultra-small TiO₂ nanoparticles disrupt microtubular networks in *Arabidopsis thaliana*. *Plant Cell Environ.* **2011**, *34*, 811–820.
- (25) Liu, Q.; Zhao, Y.; Wan, Y.; Zheng, J.; Zhang, X.; Wang, C.; Fang, X.; Lin, J. Study of the inhibitory effect of water-soluble fullerenes on plant growth at the cellular level. *ACS Nano* **2010**, *4*, 5743–5748.
- (26) Veen, B. W. The influence of mechanical impedance on the growth of maize roots. *Plant Soil* **1982**, *66*, 101–109.
- (27) Pierik, R.; Verkerke, W.; Voeseek, R.; Blom, K.; Visser, E. Thick root syndrome in cucumber (*Cucumis sativus* L.): A description of the phenomenon and an investigation of the role of ethylene. *Ann. Bot.* **1999**, *84*, 755–762.
- (28) Asli, S.; Neumann, P. Colloidal suspensions of clay or titanium dioxide nanoparticles can inhibit leaf growth and transpiration via physical effects on root water transport. *Plant Cell Environ.* **2009**, *32*, 577–584.
- (29) Nair, R.; Varghese, S. H.; Nair, B. G.; Maekawa, T.; Yoshida, Y.; Kumar, D. S. Nanoparticulate material delivery to plants. *Plant Sci.* **2010**, *179*, 154–163.
- (30) Lam, S. K.; Siu, C. L.; Hillmer, S.; Jang, S.; An, G.; Robinson, D. G.; Jiang, L. Rice SCAMP1 defines clathrin-coated, trans-golgi-located tubular-vesicular structures as an early endosome in tobacco BY-2 cells. *Plant Cell* **2007**, *19*, 296–319.
- (31) Zhang, Z. Y.; He, X.; Zhang, H. F.; Ma, Y. H.; Zhang, P.; Ding, Y. Y.; Zhao, Y. L. Uptake and distribution of ceria nanoparticles in cucumber plants. *Metallomics* **2011**, *3*, 816–822.
- (32) Esau, K. *Anatomy of Seed Plants*; John Wiley and Sons: New York, 1977.
- (33) Tanton, T. W.; Crowley, S. H. The distribution of lead chelate in the transpirational stream of higher plants. *Pestic. Sci.* **1971**, *2*, 211–213.
- (34) Haynes, R. J. Ion exchange properties of roots and ionic interactions within the root apoplast: Their role in ion accumulation by plants. *Bot. Rev.* **1980**, *46*, 75–79.
- (35) Krämer, U.; Talke, I. T.; Hanikenne, M. Transition metal transport. *FEBS Lett.* **2007**, *581*, 2263–2272.
- (36) Beattie, I. R.; Haverkamp, R. G. Silver and gold nanoparticles in plants: sites for the reduction to metal. *Metallomics* **2011**, *3*, 628–632.
- (37) Schürmann, P.; Jacquot, J. P. Plant thioredoxin systems revisited. *Annu. Rev. Plant Physiol. Plant Mol. Biol.* **2000**, *51*, 371–400.
- (38) Slewinski, T. L.; Braun, D. M. Current perspectives on the regulation of whole-plant carbohydrate partitioning. *Plant Sci.* **2010**, *178*, 341–349.